Free Radical Research, Volume 37 Number 7 (July 2003), pp. 705–712

Characterization of the High Resolution ESR Spectra of the Methoxyl Radical Adducts of 5-(diethoxyphosphoryl)-5-methyl-1-pyrroline *N*-oxide (DEPMPO)

SERGEY DIKALOV[a,*], PAUL TORDO[b], ANN MOTTEN[a] and RONALD P. MASON[a]

[a]*Laboratory of Pharmacology and Chemistry, National Institute of Environmental Health Sciences/National Institutes of Health, 111 Alexander Drive, PO Box 12233, Research Triangle Park, NC, 27709, USA;* [b]*Laboratory of Structure and Reactivity of Paramagnetic Species, University of Marseilles, F-13397 Marseilles, France*

Accepted by Professor B. Kalyanaraman

(Received 24 September 2002; In revised form 31 January 2003)

Spin-trapping investigators are largely limited by the instability of the radical adducts. Spin trap 5-(diethoxyphosphoryl)-5-methyl-1-pyrroline *N*-oxide (DEPMPO) forms very stable alkoxyl radical adducts. However, the presence of two chiral centers in the DEPMPO alkoxyl radical adduct results in two diastereomers with distinctive ESR spectra, which complicates the interpretation of the ESR spectra. We have analyzed the high resolution ESR spectra of the DEPMPO/$^{\bullet}OCH_3$ radical adduct. DEPMPO/$^{\bullet}OCH_3$ has been synthesized by the nucleophilic addition of alcohols to DEPMPO. The electron spin resonance (ESR) spectrum of DEPMPO/$^{\bullet}OCH_3$ in oxygen-free methanol solution reveals superhyperfine structure with hyperfine coupling constants as small as 0.3 G. In order to simplify the analysis of the electron spin resonance (ESR) spectrum, we synthesized the DEPMPO/$^{\bullet}OCD_3$ radical adduct. Computer simulation of the DEPMPO/$^{\bullet}OCD_3$ ESR spectrum revealed two diastereomers. Hyperfine coupling constants of γ-protons and ^{17}O from the $-OCH_3$ group were also determined. ESR spectra of DEPMPO/$^{\bullet}OCH_3$ in phosphate buffer have also been characterized. The presence of specific hyperfine couplings from the $-OCH_3$ group can be used for the unambiguous identification of the DEPMPO/$^{\bullet}OCH_3$ radical adducts. We suggest that the analysis of high resolution ESR spectra can be used for the unambiguous characterization of DEPMPO radical adducts.

Keywords: Spin trap; DEPMPO; Alkoxyl radical; Radical adduct; Oxygen-17; Superhyperfine structure

Abbreviations: DEPMPO, 5-(diethoxyphosphoryl)-5-methyl-1-pyrroline *N*-oxide; DMPO, 5,5-dimethyl-1-pyrroline *N*-oxide

INTRODUCTION

The spin-trapping technique is the most definitive method for detection of short-lived radicals.[1] This method is based on the reaction of a spin trap with radical to form a relatively stable radical adduct that can be detected by electron spin resonance (ESR).[2] The spin-trapping technique has been successfully used for detection of various oxygen-centered radicals.[1,3] However, detection of alkoxyl radicals presents several problems. In order to trap the alkoxyl radical, the spin trap has to compete with numerous radical reactions such as isomerization, β-scission, and cyclization of the alkoxyl radical.[4,5] The short lifetime and broad line width of alkoxyl radicals precludes detection by direct ESR spectroscopy. Finally, the chemical structure of the species responsible for the ESR spectra assigned to alkoxyl radical adducts must be unambiguously proven.[1,6,7]

Previously, 5-(diethoxyphosphoryl)-5-methyl-1-pyrroline *N*-oxide (DEPMPO, scheme 1) has been shown to be an effective spin trap for alkoxyl radicals.[8,9] However, interpretation of the ESR spectra was complicated by the overlapping of the two diastereomers of the radical adduct, which makes the assignment of the trapped radical very difficult.[9–11]

In this paper DEPMPO methoxyl radical adduct (DEPMPO/$^{\bullet}OCH_3$) has been synthesized

*Corresponding author. Address: Division of Cardiology, Free Radicals in Medicine Core, Emory University School of Medicine, 1639 Pierce Drive, Atlanta, GA 30322, USA. Tel.: +1-404-712-9550. Fax: +1-404-727-4080. E-mail: dikalov@emory.edu

ISSN 1071-5762 print/ISSN 1029-2470 online © 2003 Taylor & Francis Ltd
DOI: 10.1080/1071576031000097508

by an iron-catalyzed nucleophilic addition of methanol to the spin trap DEPMPO.[3,12,13] For the first time, we synthesized the DEPMPO/$^{\bullet}OCD_3$ and DEPMPO/$^{\bullet}{}^{17}OCH_3$ radical adducts. High-resolution ESR spectra of DEPMPO/$^{\bullet}OCH_3$ have been analyzed. Independent non-radical synthesis of DEPMPO/$^{\bullet}OCH_3$ provides an unequivocal assignment of the methoxyl radical adduct.

MATERIALS AND METHODS

Chemicals

Spin trap DEPMPO was obtained from OXIS (Portland, OR). DEPMPO was stored at −70°C. CD_3–OD (99.8 atom % D) and methanol-^{17}O (20 atom % ^{17}O) were from ISOTEC, Inc. (Miamisburg, OH). Methanol (CH_3OH) was obtained from Malinckrodt Baker (Paris, KY). DTPA was purchased from Sigma.

ESR Spin-trapping Experiments

The ESR spectra were recorded using an ELEXSYS ESR spectrometer (Bruker) operating at 9.78 GHz with a modulation frequency of 50 kHz and a super-high Q microwave cavity. All ESR samples were placed in a 10 mm flat cell. The ESR instrumental settings were as follows: field sweep, 120 G; microwave frequency, 9.78 GHz; microwave power, 20 mW; modulation amplitude, 0.2 G; conversion time, 656 ms; time constant, 656 ms; and receiver gain, 1×10^5, 4096 points, 20 scans. ESR spin-trapping experiments were done at least three times.

Synthesis of Methoxyl Radical Adducts

DEPMPO/$^{\bullet}OCH_3$ radical adduct was synthesized by nucleophilic addition in a non-aqueous solution of methanol containing 0.5 mM $FeCl_3$.[3] In order to synthesize the DEPMPO/$^{\bullet}{}^{17}OCH_3$ radical adduct, ^{17}O–methanol was used (it contained 20% CH_3–^{17}OH). In order to synthesize the DEPMPO/$^{\bullet}OCD_3$ radical adduct, CD_3OD was used (99.8% D). The reaction was initiated in the flat cell by adding the DEPMPO (50 mM) to an argon-bubbled non-aqueous solution of $FeCl_3$ in methanol.

Computer Simulation

Computer simulations and spin-trap data base searches were performed using a program that is available to the public through the Internet (http://epr.niehs.nih.gov/). The details of this computer simulation program have been described elsewhere.[14] Hyperfine coupling constants are expressed as an average of ESR parameters obtained from computer simulations of three experimental spectra (Table I). Hyperfine coupling constants obtained from simulations of different ESR spectra varied not more than 0.05 G.

RESULTS

Synthesis of DEPMPO-methoxyl Radical Adducts by Nucleophilic Addition of Methanol to DEPMPO

Previously, it was shown that methoxyl radical adducts can be synthesized by a nucleophilic addition of methanol to the spin trap catalyzed by ferric ions.[3,1,213] This reaction has been used in order to synthesize DEPMPO methoxyl radical adducts. Scheme 1 shows the proposed mechanism of this reaction.

The ESR spectrum of a methanol solution of DEPMPO in the presence of $FeCl_3$ using a modulation amplitude of 1.0 G showed significant formation of a radical adduct (Fig. 1A). This spectrum consists of many broad lines with line widths of about 2 G. The ESR spectrum of a nitrogen-bubbled methanol solution of DEPMPO with $FeCl_3$ scanned at modulation amplitude 0.2 G contains a superhyperfine structure with hyperfine coupling constants as small as 0.3 G (Fig. 1B). This spectrum persisted for many hours. The ESR spectrum obtained after 20 h (Fig. 1C) was only slightly different from the initial spectrum (Fig. 1B). The ESR spectrum of the methanol solution of DEPMPO with $FeCl_3$ diluted fourfold by phosphate buffer (Fig. 1D) was significantly different from the methanol spectrum (Fig. 1B). The DEPMPO/$^{\bullet}OCH_3$ radical adduct in phosphate buffer was not as stable as in methanol. Twenty hours later, the ESR spectrum of DEPMPO/$^{\bullet}OCH_3$ in phosphate buffer had one-half the ESR amplitude of the initial spectrum (Fig. 1D and E). Moreover, some ESR lines had disappeared from the spectrum after 20 h, implying that at least one of the radical adducts had totally decayed during the 20-h incubation.

In order to reveal the contribution of protons of the methoxyl group in the ESR spectrum of DEPMPO/$^{\bullet}OCH_3$ (Fig. 2A), we synthesized DEPMPO/$^{\bullet}OCD_3$ radical adduct (Fig. 2B). For a detailed comparison we plotted half of the ESR spectra of DEPMPO/$^{\bullet}OCH_3$ and DEPMPO/$^{\bullet}OCD_3$ (Fig. 2C and D). The ESR spectra of DEPMPO/$^{\bullet}OCH_3$ and DEPMPO/$^{\bullet}OCD_3$ were found to be significantly different (Fig. 2C and D). The ESR spectrum of DEPMPO/$^{\bullet}OCD_3$ contains a smaller number of lines, and the distribution of ESR intensities was very different from DEPMPO/$^{\bullet}OCH_3$, which confirms the contribution of protons of the methoxyl group to the ESR spectrum of DEPMPO/$^{\bullet}OCH_3$.

TABLE I Hyperfine coupling constants of methoxyl radical adducts (G)

Radical adduct	N	Hβ	H_{OCH_3}	H_{CH_3}	$Hγ^3$	$Hγ^{3,4}$	^{31}P	^{17}O	Experimental condition
DMPO/$^{\bullet}OCH_3$	14.45	10.61			1.35			6.51	DMPO + Fe^{3+} in 5% CH_3OH (reference 3)
DMPO/$^{\bullet}OCH_3$	12.93	6.55			1.79			6.45	DMPO + Fe^{3+} in CH_3OH (20% $CH_3-{}^{17}OH$)
DEPMPO/$^{\bullet}OCH_3$	12.91	7.18			1.27		46.57		DEPMPO + $Pb(OAc)_4$ in CH_3OH (reference 9)
	13.04	7.62			1.7		39.72		
DEPMPO/$^{\bullet}OCH_3$	12.88	7.13	0.52	0.39	1.23	0.30 0.86 0.46	46.49		DEPMPO + Fe^{3+} in CH_3OH
	13.01	7.57	0.34	0.46	1.69	0.39 0.38	39.62		
DEPMPO/$^{\bullet}{}^{17}OCH_3$	12.87	7.11	0.52	0.39	1.23	0.30 0.86 0.46	46.48	5.84	DEPMPO + Fe^{3+} in CH_3OH (20% $CH_3-{}^{17}OH$)
	13.00	7.55	0.34	0.46	1.69	0.39 0.38	39.60	5.37	
DEPMPO/$^{\bullet}OCD_3$	12.88	7.13	0.08	0.36	1.23	0.32 0.80 0.48	46.48		DEPMPO + Fe^{3+} in CD_3OD
	13.01	7.59	0.05	0.47	1.69	0.39 0.37	39.61		
DEPMPO/$^{\bullet}OCH_3$	13.42	9.11	0.41	0.39	1.08	0.34 0.72 0.41	47.82		DEPMPO + Fe^{3+} in CH_3OH + 75% PB
	13.57	8.21	0.30	0.48	1.68	0.44 0.35	40.51		
DEPMPO/$^{\bullet}OCH_3$	13.52	9.51	0.39	0.37	1.04	0.31 0.72 0.41	47.54		DEPMPO + Fe^{3+} in CH_3OH + 99% PB
	13.64	8.27	0.35	0.48	1.68	0.42 0.35	40.63		

Computer Analysis of Hyperfine Couplings from γ-protons of DEPMPO-methoxyl Radical Adducts

Previously, it was reported that the ESR spectrum of the DMPO-methoxyl radical adduct has a resolved hyperfine coupling constant of 1.33 G from the γ-proton at position 3.[3,15] The ESR spectrum of the DEPMPO-methoxyl radical adduct contains a great number of ESR lines with a hyperfine coupling constant as small as 0.3 G that confirms the contribution of many γ-protons of the DEPMPO-methoxyl radical adduct to the superhyperfine structure of the ESR spectrum.

Scheme 1 shows the chemical structures of two diastereomers of the DEPMPO/$^{\bullet}OCH_3$ radical adduct. It is known that radical adduct diastereomers can have a distinctive ESR spectrum.[12,16,17] Figure 1E shows mainly one diastereomer of DEPMPO/$^{\bullet}OCH_3$. Comparison of the ESR spectra in Fig. 1D and E clearly disassociates the ESR spectra of the two diastereomers. The low-field component of the ESR spectrum in Fig. 1E originates from only one diastereomer of DEPMPO/$^{\bullet}OCH_3$ present. Components from the center of the ESR spectrum are associated with the second diastereomer of the DEPMPO/$^{\bullet}OCH_3$ radical adduct. However, ESR spectra of the diastereomers of DEPMPO/$^{\bullet}OCH_3$ are considerably overlapped, complicating the analysis of the experimental spectrum (Fig. 1B and D).

In order to analyze the hyperfine couplings from the γ-proton of the DEPMPO-methoxyl radical adduct, we used well defined components of the ESR spectra associated with a particular diastereomer. The low-field component of the ESR spectrum of the first diastereomer has been reconstructed by mirror imaging of the low-field portion of that component (Fig. 3A and C). The low-field component of the high-field half of the ESR spectrum of the second diastereomer has been reconstructed by mirror imaging of the low-field portion of that component (Fig. 3E and G). The analysis of the hyperfine couplings from γ-protons was done first for DEPMPO/$^{\bullet}OCD_3$ (Fig. 3A and E) because of the smaller number of γ-protons.

Computer simulation of the low-field component of the ESR spectrum of the first diastereomer of DEPMPO/$^{\bullet}OCD_3$ required seven γ-protons (Fig. 3B). Hyperfine coupling constants from five γ-protons were very similar while hyperfine coupling constants of two other γ-protons were 2-fold and 3-fold higher, respectively (Table I). Large hyperfine coupling constants have been tentatively assigned to the corresponding protons at position 4 and position 3 (Scheme 1) based on their similarity with the DMPO radical adducts.[1,18] Computer simulation of the low-field component of the ESR spectrum of the first diastereomer of DEPMPO/$^{\bullet}OCH_3$ required ten

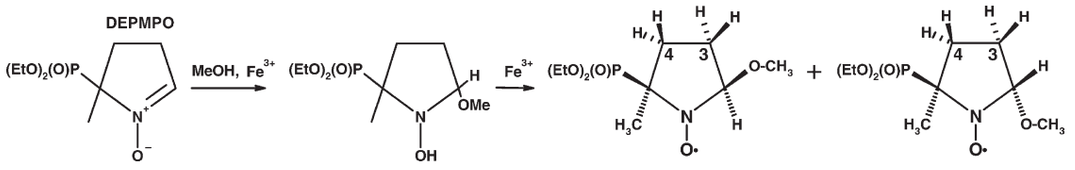

SCHEME 1 Proposed mechanism of nucleophilic addition of methanol to DEPMPO.

γ-protons (Fig. 3D), including three protons from the methoxyl group (Scheme 1).

Computer simulation of the component of the ESR spectrum of the second diastereomer of DEPMPO/$^{\bullet}OCD_3$ required six γ-protons (Fig. 3E). Hyperfine coupling constants from five γ-protons were very similar while one hyperfine-coupling constant was 4-fold higher and was tentatively assigned to a proton at position 3 (Table I). Computer simulation of the component of the ESR spectrum of the second diastereomer of DEPMPO/$^{\bullet}OCH_3$ required 9 γ-protons (Fig. 3H), including 3 protons from the methoxyl group (Scheme 1).

It is important to note that the hyperfine-coupling constants of γ-protons of both diastereomers of DEPMPO/$^{\bullet}OCD_3$ were found to be nearly identical to DEPMPO/$^{\bullet}OCH_3$, which supports the correctness of the computer simulation and confirms the hyperfine-coupling constants of the γ-protons (Table I).

Computer Simulation of ESR Spectra of DEPMPO-methoxyl Radical Adducts

As shown previously, the ESR spectrum of the DEPMPO-methoxyl radical adducts is a superposition of the ESR spectra of two diastereomers. Therefore, the ESR spectrum of the DEPMPO/$^{\bullet}OCD_3$ radical adduct (Fig. 4A) has been simulated as a combination of two diastereomers of the radical adduct (Fig. 4B). The composite simulation (Fig. 4B) consisted of two ESR spectra (Fig. 4C and D) with molar portions of 60 and 40%. The ESR spectrum of the first diastereomer (Fig. 4C) is a doublet ($a^{P} = 46.48$ G) of sextets ($a^{N} = 12.87$ G and $a_{\beta}^{H} = 7.11$ G) (Table I). The ESR spectrum of

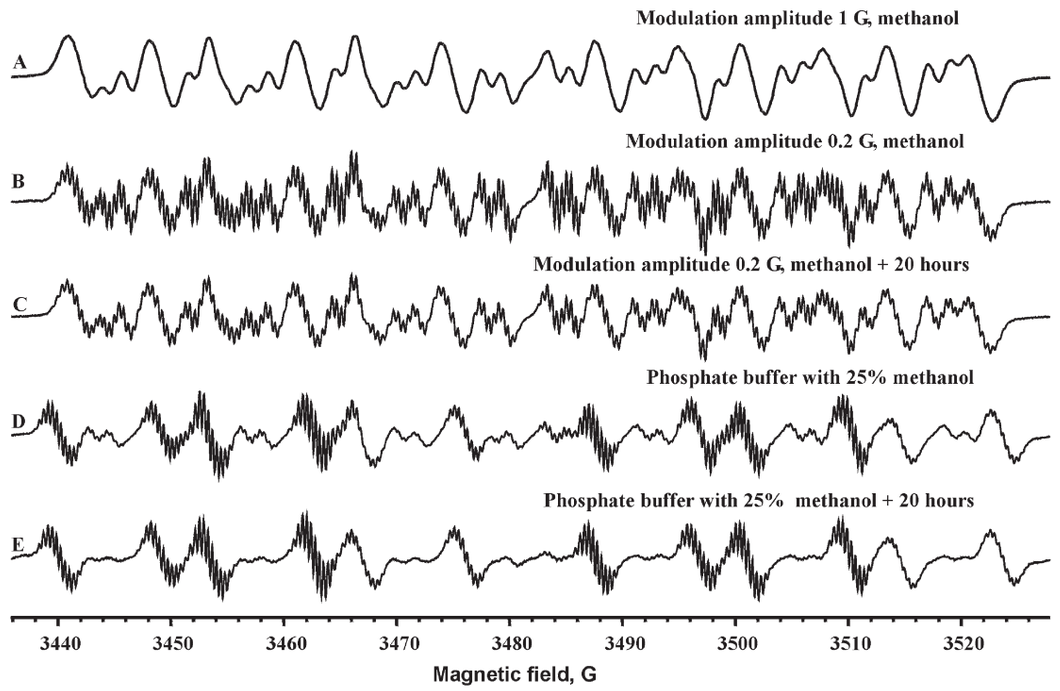

FIGURE 1 ESR spectra of DEPMPO methoxyl radical adduct in methanol and phosphate buffer. (A) ESR spectrum of methanol solution of DEPMPO (60 mM) with $FeCl_3$ (0.2 mM) scanned at modulation amplitude 1 G. (B) ESR spectrum of N_2-bubbled methanol solution of DEPMPO (60 mM) with $FeCl_3$ (0.2 mM) scanned at modulation amplitude 0.2 G. (C) The same as (B) but 20 h later. (D) ESR spectrum of N_2-bubbled phosphate buffer with 10 mM DTPA plus methanol solution (25%) containing DEPMPO (60 mM) with $FeCl_3$ (0.2 mM) obtained at modulation amplitude 0.2 G. (E) The same as (D) but 20 h later at 2-fold higher gain.

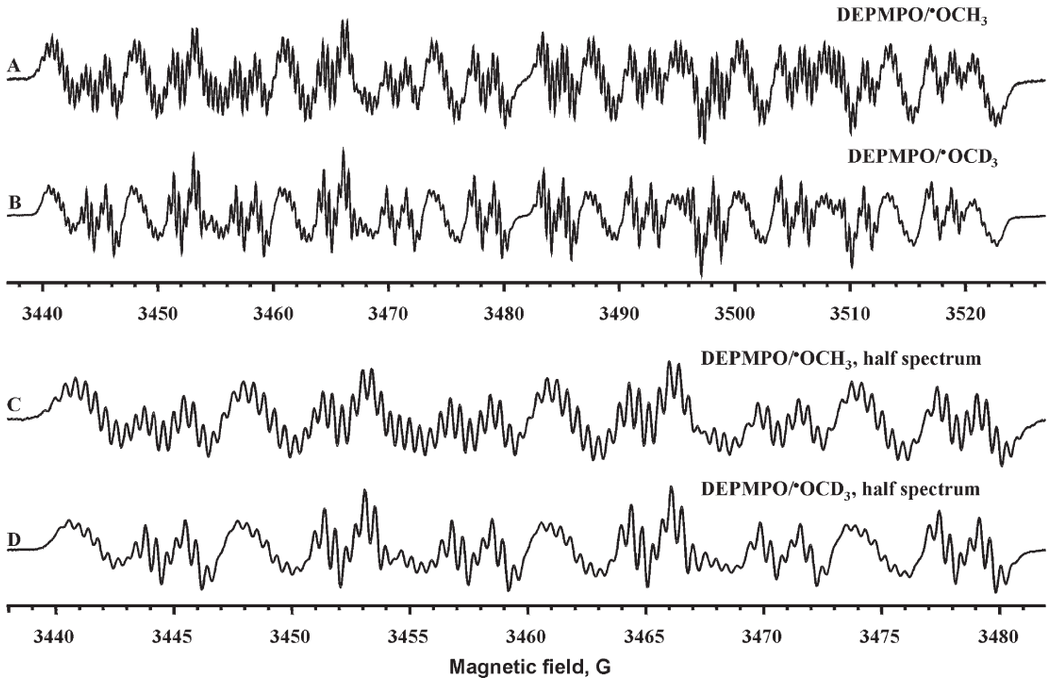

FIGURE 2 ESR spectra of DEPMPO/$^{\bullet}OCH_3$ and DEPMPO/$^{\bullet}OCD_3$. (A) ESR spectrum of N_2-bubbled CH_3OH solution of DEPMPO (60 mM) with $FeCl_3$ (0.2 mM). (B) ESR spectrum of N_2-bubbled CD_3OD solution of DEPMPO (60 mM) with $FeCl_3$ (0.2 mM). (C) Half of the ESR spectrum of N_2-bubbled CH_3OH solution of DEPMPO (60 mM) with $FeCl_3$ (0.2 mM). (D) Half of the ESR spectrum of N_2-bubbled CD_3OD solution of DEPMPO (60 mM) with $FeCl_3$ (0.2 mM). ESR settings were as described in "Materials and Methods" section.

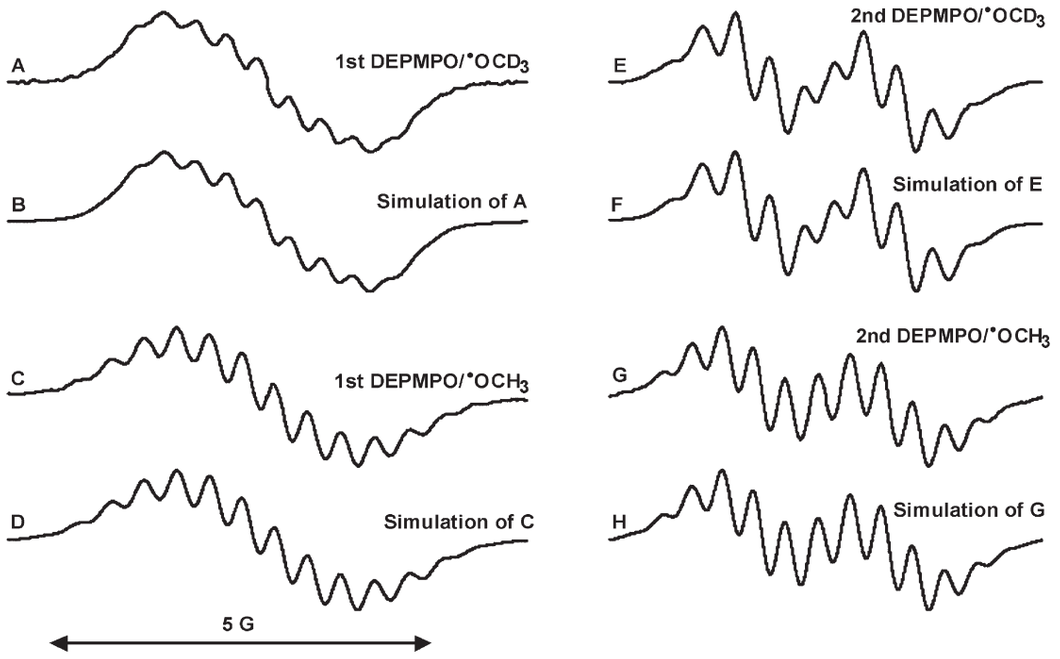

FIGURE 3 Computer analysis of hyperfine couplings from γ-protons of DEPMPO-methoxyl radical adducts. (A) Low-field component of the ESR spectrum of the first diastereomer of DEPMPO/$^{\bullet}OCD_3$ reconstructed by mirror imaging of the low-field portion of that component. (B) Computer simulation of spectrum (A). (C) Low-field component of the ESR spectrum of the first diastereomer of DEPMPO/$^{\bullet}OCH_3$ reconstructed by mirror imaging of the low-field portion of that component. (D) Computer simulation of spectrum (C). (E) Low-field component of the high-field half of the ESR spectrum of the second diastereomer of DEPMPO/$^{\bullet}OCD_3$ reconstructed by mirror imaging of the low-field portion of that component. (F) Computer simulation of spectrum (E). (G) Low-field component of the high-field half of the ESR spectrum of the second diastereomer of DEPMPO/$^{\bullet}OCH_3$ reconstructed by mirror imaging of the low-field portion of that component. (H) Computer simulation of spectrum (G).

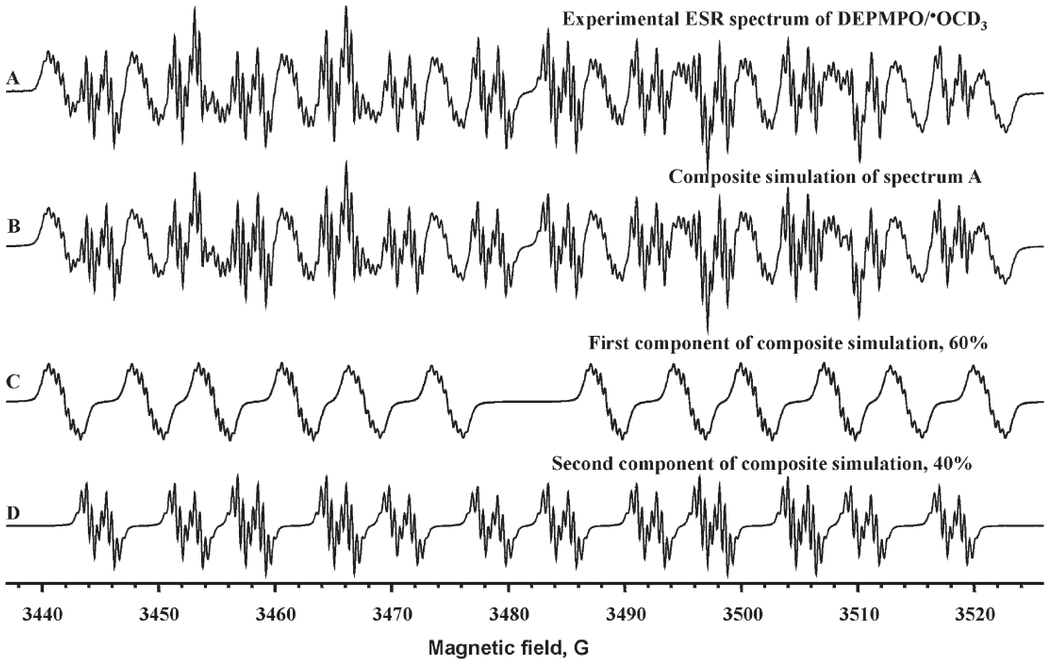

FIGURE 4 Computer simulation of DEPMPO/•OCD_3 ESR spectrum. (A) ESR spectrum of N_2-bubbled CD_3OD solution of DEPMPO (60 mM) with $FeCl_3$ (0.2 mM). (B) Composite computer simulation of spectrum (A). (C) Computer simulation of the first diastereomer of DEPMPO/•OCD_3 in spectrum (A). (D) Computer simulation of the second diastereomer of DEPMPO/•OCD_3 in spectrum (A).

the second diastereomer (Fig. 4D) is also a doublet ($a^P = 39.60$ G) of sextets ($a^N = 13.00$ G and $a_\beta^H = 7.55$ G) with an obvious 1.69 G splitting on the γ-proton (Table I).

The ESR spectrum of the DEPMPO/•OCH_3 radical adduct (Fig. 5A) has been simulated similarly to DEPMPO/•OCD_3 (Fig. 4A) as a combination of two diastereomers of the radical

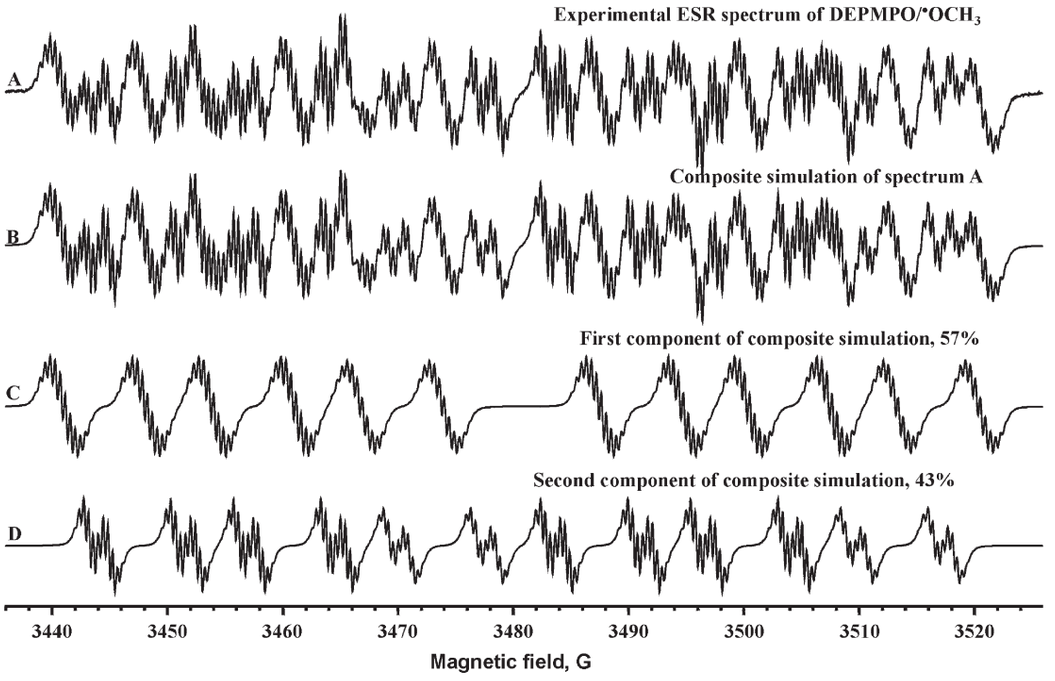

FIGURE 5 Computer simulation of DEPMPO/•OCH_3 ESR spectrum. (A) ESR spectrum of N_2-bubbled CH_3OH solution of DEPMPO (60 mM) with $FeCl_3$ (0.2 mM). (B) Composite computer simulation of spectrum (A). (C) Computer simulation of the first diastereomer of DEPMPO/•OCH_3 in spectrum (A). (D) Computer simulation of the second diastereomer of DEPMPO/•OCH_3 in spectrum (A).

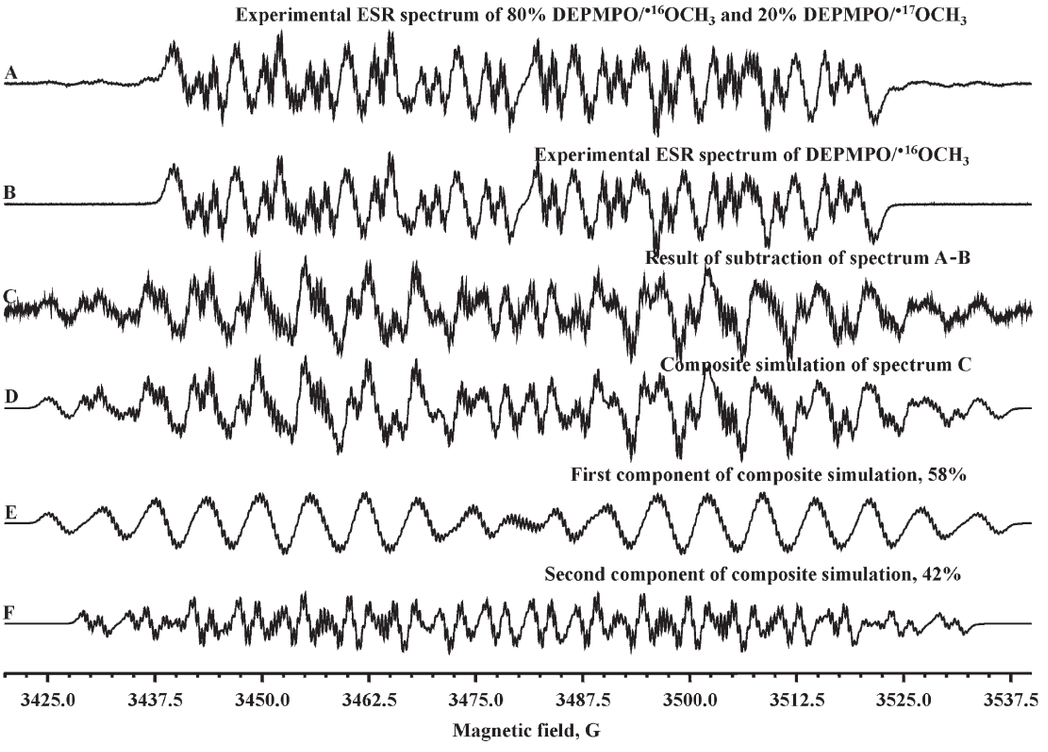

FIGURE 6 Computer simulation of DEPMPO/$^{\bullet 17}OCH_3$ ESR spectrum. (A) ESR spectrum of N_2-bubbled $CH_3-{}^{17}OH$ solution of DEPMPO (60 mM) with $FeCl_3$ (0.2 mM). (B) ESR spectrum of N_2-bubbled $CH_3-{}^{16}OH$ solution of DEPMPO (60 mM) with $FeCl_3$ (0.2 mM). (C) ESR spectrum obtained by the subtraction of spectrum (B) from spectrum (A). (D) Composite computer simulation of spectrum (C). (E) Computer simulation of the first diastereomer of DEPMPO/$^{\bullet 17}OCH_3$ in spectrum (C). (F) Computer simulation of the second diastereomer of DEPMPO/$^{\bullet 17}OCH_3$ in spectrum (C).

adduct (Fig. 5B). The composite simulation (Fig. 5B) consisted of two ESR spectra (Fig. 5C and D) with molar portions of 57 and 43%. The ESR spectrum of the first diastereomer (Fig. 5C) is a doublet ($a^P = 46.48$ G) of sextets ($a^N = 12.87$ G and $a^H_\beta = 7.11$ G) with 10 γ-protons (Table I). The ESR spectrum of the second diastereomer (Fig. 4D) is also a doublet ($a^P = 39.60$ G) of sextets ($a^N = 13.00$ G, $a^H_\beta = 7.55$ G) with an obvious 1.69 G splitting and a total of nine hyperfine splittings from γ-protons (Table I).

Figures 4 and 5 show a significant difference between the ESR spectra of the two diastereomer DEPMPO-methoxyl radical adducts. It is due to very distinct hyperfine coupling constants of the phosphorous (46.48 vs. 39.60 G), β-proton (7.11 vs. 7.55 G), and γ-proton (1.23 vs. 1.69 G). The significant difference in the ESR spectra of the diastereomers results from the distinct conformations of these molecules.[16,17]

Previously, it was shown that the hyperfine splitting from ^{17}O of the methoxyl radical adducts is very specific and can be used to distinguish –OH, –OOH, and $-OCH_3$ radical adducts.[3,19] Therefore, we have analyzed the ESR spectrum of the DEPMPO/$^{\bullet 17}OCH_3$ radical adduct (Fig. 6). Figure 6A shows the ESR spectrum of a N_2-bubbled $CH_3-{}^{17}OH$ (20-atom % ^{17}O) solution of DEPMPO with $FeCl_3$. The ESR spectrum obtained with $CH_3-{}^{17}OH$ revealed a specific hyperfine splitting from ^{17}O on the low-field and high-field wings of the ESR spectrum (Fig. 6A). Figure 6B shows the ESR spectrum of a N_2-bubbled $CH_3-{}^{16}OH$ solution of DEPMPO with $FeCl_3$, which has no additional lines from hyperfine splitting on ^{17}O. In order to reveal the ESR spectrum of DEPMPO/$^{\bullet 17}OCH_3$, we have subtracted ESR spectrum 6B from spectrum 6A. The result of this subtraction has been shown in Fig. 6C. Computer simulation (Fig. 6D) consisted of two diastereomers of DEPMPO/$^{\bullet 17}OCH_3$ with contributions of 58% (Fig. 6E) and 42% (Fig. 6F). The hyperfine coupling constants of ^{17}O are shown in Table I. The DEPMPO/$^{\bullet 17}OCH_3$ radical adduct has been described for the first time. The hyperfine coupling constants of ^{17}O are significantly different for the two diastereomers of DEPMPO/$^{\cdot 17}OCH_3$ (5.84 vs. 5.37 G). It is important to note that all other hyperfine coupling constants (N, P, β-proton, γ-protons) of DEPMPO/$^{\bullet 17}OCH_3$ were identical to DEPMPO/$^{\bullet 16}OCH_3$ (Table I).

Computer simulation of the ESR spectrum from Fig. 6A revealed 80% DEPMPO/$^{\bullet 16}OCH_3$ and 20% DEPMPO/$^{\bullet 17}OCH_3$, which is consistent

with the content of ^{17}O in ^{17}O-labeled methanol (20-atom % ^{17}O).

DISCUSSION

This paper presents the analysis of the high resolution ESR spectra of the DEPMPO/$^{\bullet}OCH_3$ radical adduct synthesized by the nucleophilic addition of alcohols to DEPMPO. Computer simulation of the DEPMPO/$^{\bullet}OCH_3$ ESR spectrum revealed two diastereomers (Table I). For the first time hyperfine coupling constants of methoxyl protons and ^{17}O from the $-OCH_3$ group have been determined (Table I).

The presence of superhyperfine structure in the DEPMPO/$^{\bullet}OCH_3$ ESR spectrum is quite remarkable. The resolved hyperfine couplings from the $-OCH_3$ group are particularly useful for the unambiguous identification of the DEPMPO/$^{\bullet}OCH_3$ radical adducts.

Identification of the trapped radical is usually limited by the lack of specificity of the ESR spectra of particular radical adducts. Nitroso spin traps form radical adducts with resolved hyperfine couplings from trapped alkyl radicals.[1] However, radical adducts of nitroso spin traps with oxygen-centered radicals are not stable.[1] Nitrone spin traps such as DMPO and DEPMPO form stable radical adducts with alkoxyl radicals.[1] However, identification of the structure of the trapped alkoxyl radical is very difficult. The DMPO alkoxyl radical adducts do not provide resolved hyperfine couplings from the alkyl part of their radical adducts. Interestingly, the DEPMPO/$^{\bullet}OCH_3$ radical adduct revealed resolved hyperfine couplings from the alkyl part of the trapped $CH_3O^{\bullet}$ radical, which makes the ESR spectrum of the DEPMPO radical adduct unique and unambiguous for the detection of alkoxyl radicals.

The high stability of DEPMPO radical adducts and the presence of specific hyperfine couplings from the trapped alkoxyl radical can be used for the unambiguous identification of alkoxyl radical adducts. We suggest that high-resolution ESR spectra of DEPMPO radical adducts may be an important tool for their characterization.

References

[1] Janzen, E.G. and Haire, D.L. (1990) "Two decades of spin trapping", *Adv. Free Radic. Chem.* **1**, 253–295.

[2] Janzen, E.G. (1971) "Spin trapping", *Acc. Chem. Res.* **4**, 31–40.

[3] Dikalov, S.I. and Mason, R.P. (1999) "Reassignment of organic peroxyl radical adducts", *Free Radic. Biol. Med.* **27**, 864–872.

[4] Ledwith, A., Russell, P.J. and Sutcliffe, L.H. (1973) "Alkoxy radical intermediates in the thermal and photochemical oxidation of alcohols", *Proc. R. Soc. Lond. A.* **332**, 151–166.

[5] Grossi, L., Strazzari, S., Gilbert, B.C. and Whitwood, A.C. (1998) "Oxiranylcarbinyl radicals from allyloxyl radical cyclization: characterization and kinetic information via ESR spectroscopy", *J. Org. Chem.* **63**, 8366–8372.

[6] Kotake, Y. and Janzen, E.G. (1991) "Decay and fate of the hydroxyl radical adduct of.alpha.-phenyl-*N*-tert-butylnitrone in aqueous media", *J. Am. Chem. Soc.* **113**, 9503–9506.

[7] Janzen, E.G., Krygsman, P.H., Lindsay, D.A. and Haire, D.L. (1990) "Detection of alkyl, alkoxyl, and alkyperoxyl radicals from the thermolysis of azobis(isobutyronitrile) by ESR/spin trapping. Evidence for double spin adducts from liquid-phase chromatography and mass spectroscopy", *J. Am. Chem. Soc.* **112**, 8279–8284.

[8] Frejaville, C., Karoui, H., Tuccio, B., Le Moigne, F., Culcasi, M., Pietri, S., Lauricella, R. and Tordo, P. (1994) "5-Diethoxyphosphoryl-5-methyl-1-pyrroline *N*-oxide (DEPMPO)—a new phosphorylated nitrone for the efficient *in vitro* and *in vivo* spin-trapping of oxygen-centered radicals", *J. Chem. Soc. Chem. Commun.* **15**, 1793–1794.

[9] F. Chalier. PhD Thesis, University of Marseilles, Marseilles, France.

[10] Frejaville, C., Karoui, H., Tuccio, B., Le Moigne, F., Culcasi, M., Pietri, S., Lauricella, R. and Tordo, P. (1995) "5-(Diethoxyphosphoryl)-5-methyl-1-pyrroline *N*-oxide—a new efficient phosphorylated nitrone for the *in vitro* and *in vivo* spin trapping of oxygen-centered radicals", *J. Med. Chem.* **38**, 258–265.

[11] Vasquez-Vivar, J., Hogg, N., Marthasek, P., Karoui, H., Tordo, P., Pritchard, K.A. and Kalyanaraman, B. (1999) "Effect of redox-active drugs on superoxide generation from nitric oxide synthases: biological and toxicological implications", *Free Radic. Res.* **31**, 607–617.

[12] Makino, K., Hagiwara, T., Hagi, A., Nishi, M. and Murakami, A. (1990) "Cautionary note for DMPO spin trapping in the presence of iron ion", *Biochem. Biophys. Res. Commun.* **172**, 1073–1080.

[13] Nishi, M., Hagi, A., Ide, H., Murakami, A. and Makino, K. (1992) "Comparison of 2,5,5-trimethyl-1-pyrroline-*N*-oxide (M_3PO) and 3,3,5,5-tetramethyl-pyrroline-*N*-oxide (M_4PO) with 5,5-dimethyl-1-pyrroline-*N*-oxide (DMPO) as spin traps", *Biochem. Int.* **27**, 651–659.

[14] Duling, D.R. (1994) "Simulation of multiple isotropic spin-trap ESR spectra", *J. Magn. Res. Series B* **104**, 105–110.

[15] Hanna, P.M., Chamulitrat, W. and Mason, R.P. (1992) "When are metal ion-dependent hydroxyl and alkoxyl radical adducts of 5,5-dimethyl-1-pyrroline *N*-oxide artifacts?", *Arch. Biochem. Biophys.* **296**, 640–644.

[16] Kotake, Y., Kuwata, K. and Janzen, E.G. (1979) "Electron spin resonance spectra of diastereomeric nitroxyls produced by spin trapping hydroxyalkyl radicals", *J. Phys. Chem.* **83**, 3024–3029.

[17] Dikalov, S.I. and Mason, R.P. (2001) "Spin trapping of polyunsaturated fatty acid-derived peroxyl radicals. Reassignment to alkoxyl radical adducts", *Free Radic. Biol. Med.* **30**, 187–197.

[18] Haire, D.L., Oehler, U.M., Goldman, H.D., Dudley, R.L. and Janzen, E.G. (1988) "The 1st H-1 and N-14 ENDOR spectra of an oxygen-centered radical adduct of DMPO-type nitrones", *Can. J. Chem.* **66**, 2395–2402.

[19] Mottley, C., Connor, H.D. and Mason, R.P. (1986) "[^{17}O]Oxygen hyperfine structure for the hydroxyl and superoxide radical adducts of the spin traps DMPO, PBN and 4-POBN", *Biochem. Biophys. Res. Commun.* **141**, 622–628.